



Received 23 June 2017

Accepted 3 July 2017

Edited by W. T. A. Harrison, University of
Aberdeen, Scotland**Keywords:** crystal structure; isoflavone; chro-
mone.**CCDC reference:** 1453086**Supporting information:** this article has
supporting information at journals.iucr.org/e

Structure of 7-hydroxy-3-(2-methoxyphenyl)-2-trifluoromethyl-4*H*-chromen-4-one

John Nicolson Low,^{a*} Ligia R. Gomes,^{b,c} Alexandra Gaspar^d and Fernanda Borges^d

^aDepartment of Chemistry, University of Aberdeen, Meston Walk, Old Aberdeen, AB24 3UE, Scotland, ^bFP-ENAS-Faculdade de Ciências de Saúde, Escola Superior de Saúde da UFP, Universidade Fernando Pessoa, Rua Carlos da Maia, 296, P-4200-150 Porto, Portugal, ^cREQUIMTE, Departamento de Química e Bioquímica, Faculdade de Ciências da Universidade do Porto, Rua do Campo Alegre, 687, P-4169-007, Porto, Portugal, and ^dCIQ/Departamento de Química e Bioquímica, Faculdade de Ciências, Universidade do Porto, 4169-007 Porto, Portugal. *Correspondence e-mail: jnlow111@gmail.com

Herein, the synthesis and crystal structure of 7-hydroxy-3-(2-methoxyphenyl)-2-trifluoromethyl-4*H*-chromen-4-one, C₁₇H₁₁F₃O₄, are reported. This isoflavone is used as a starting material in the preparation an array of potent and competitive FPR antagonists. The pyran ring significantly deviates from planarity and the dihedral angle between the benzopyran mean plane and that of the exocyclic benzene ring is 88.18 (4)°. In the crystal, O—H···O hydrogen bonds connect the molecules into *C*(8) chains propagating in the [010] direction.

1. Chemical context

Isoflavones are a subclass of a larger chemical family, the flavonoids, being characterized by possessing a 3-phenylchromen-4-one (3-phenyl-1,4-benzopyrone) backbone instead of the 2-phenylchromen-4-one (2-phenyl-1,4-benzopyrone) structure of flavanones and flavones (Szeja *et al.*, 2016). Dietary isoflavones are secondary metabolites that occur in plants of the Fabaceae family and as such are present in soy beans, soy foods and legumes. The health benefits of isoflavones have been linked to cholesterol-reducing, anti-inflammatory, chemotherapeutic and antioxidant properties (Jie *et al.*, 2016). However, the best known property of isoflavones is related to their phytoestrogenic activity (Vitale *et al.*, 2013). More recently, isoflavones of synthetic origin have been shown to be potent and competitive antagonists of formyl peptide receptors (FPRs), playing an important role in the regulation of inflammatory processes (Schepetkin *et al.*, 2014).

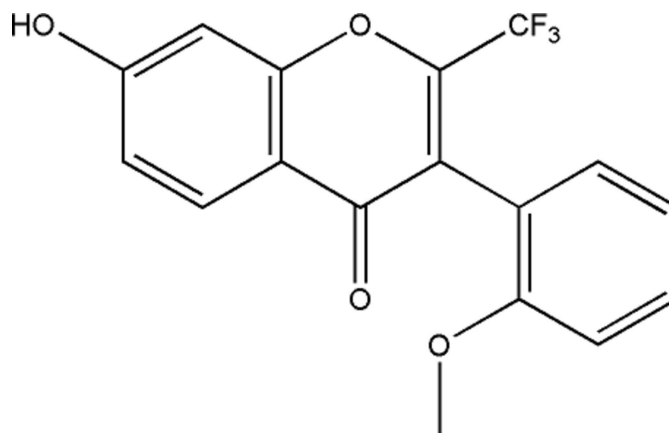
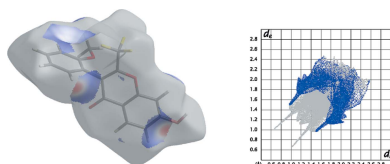


Table 1

Deviations (in Å) of the pyran ring atoms and attached atoms from the mean plane of the chromone benzene ring.

Atom	O1	C2	C3'	C4	C21	C31	O4
Distance	-0.0092 (18)	-0.243 (2)	-0.380 (2)	-0.155 (2)	-0.372 (3)	-0.805 (3)	-0.1267 (16)

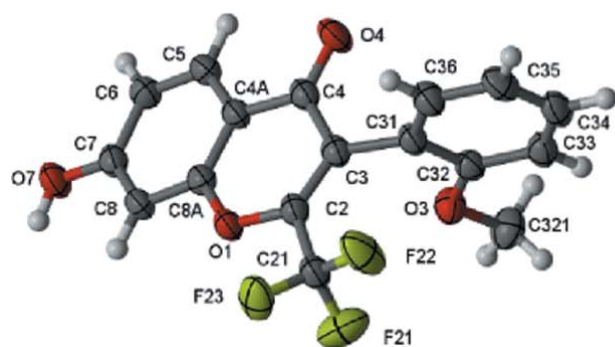
Herein we describe the synthesis and characterization of an isoflavone, 7-hydroxy-3-(2-methoxyphenyl)-2-trifluoromethyl-4*H*-chromen-4-one, **1**, a precursor used in the preparation of relevant FPRs antagonists.

2. Structural commentary

The molecular structure of **1** is shown in Fig. 1 (left). This compound consists of a chromone core with several substituents, *viz.* a trifluoromethyl group at position 2, a 2-(methoxy)phenyl at position 3 and finally an hydroxy group at position 7 of the chromone ring.

The pyran ring is not planar as the weighted average absolute torsion angle is 6.77 (7)°; for planarity this should be below 5.00° (Domenicano *et al.*, 1975). In fact, as a Cremer & Pople puckering analysis shows, the pyran ring has a twist-boat pucker with puckering amplitude $Q = 0.1085$ (13) Å, $\theta = 90.0$ (7)° and $\varphi = 148.6$ (7)°. The fused aromatic benzopyran ring system shows a slight distortion from planarity as a result of the puckering of the pyran ring. The dihedral angle between the pyran ring and the exocyclic benzene ring is 89.26 (6)°. The mean plane of the ten atoms of the benzopyran ring system was used to evaluate the degree of twisting of the 2-methoxyphenyl ring in relation to the chromone as depicted in Fig. 1 (right). The dihedral angle between the benzopyran mean plane and the exocyclic benzene ring is 88.18 (4)°; the major rotation is around the C3–C31 bond, which has sp^3 character, with a bond length of 1.4983 (17) Å. This conformation is to be expected and probably results from minimization of the steric hindrance between the 2-methoxy substituent of the exocyclic benzene ring with the voluminous –CF₃ group and/or the oxo oxygen atom of the chromone ring.

Regarding the mean plane involving the benzopyran atoms, it is found that atoms O1 and C3 lie more than 0.1 Å out of it


Figure 1

The molecular structure of **1** (left) and (right) the rotation of the exocyclic benzene relative to the benzopyran best plane [dihedral angle = 88.18 (4)°]. Displacement ellipsoids are drawn at the 70% probability level.

Table 2

Hydrogen-bond geometry (Å, °).

$D-H\cdots A$	$D-H$	$H\cdots A$	$D\cdots A$	$D-H\cdots A$
O7–H7 \cdots O4 ⁱ	0.87 (2)	1.79 (2)	2.6416 (13)	166 (2)
C6–H6 \cdots O3 ⁱⁱ	0.95	2.59	3.4309 (16)	148
C36–H36 \cdots O7 ⁱⁱⁱ	0.95	2.49	3.3886 (18)	157
C8–H8 \cdots Cg3 ^{iv}	0.95	2.93	3.5972 (14)	128
C321–H32b \cdots Cg3 ^v	0.98	2.75	3.6348 (17)	150

Symmetry codes: (i) $-x + \frac{1}{2}, y - \frac{1}{2}, z$; (ii) $-x, -y + 1, -z + 1$; (iii) $-x + 1, -y + 1, -z + 1$; (iv) $x, -y - \frac{3}{2}, z - \frac{1}{2}$; (v) $x - \frac{3}{2}, y, -z - \frac{1}{2}$.

[the perpendicular vectors having values of 0.1039 (9) Å and –0.1398 (10) Å, respectively], showing again that the benzopyran ring itself does not show the typical planarity observed for similar chromone and coumarin structures (*e.g.* Gomes *et al.*, 2016; Reis *et al.*, 2013) in which the pyran and benzopyran ring systems are essentially planar. As can be seen in Table 1, the atoms of the pyran ring lie below the mean plane of the chromone benzene ring.

3. Supramolecular features

Details of the hydrogen-bonding interactions are given in Table 2. The O7–H7 \cdots O4($\frac{1}{2} - x, -\frac{1}{2} + y, z$) link forms a $C(8)$ chain, which runs parallel to the b axis. This is formed by the action of the c -glide plane at $y = \frac{1}{4}$, Fig. 2.

The molecules are linked into alternating pairs of dimers to form a ladder. The C36–H36 \cdots O7($1 - x, 1 - y, 1 - z$) interaction forms an $R_2^2(20)$ centrosymmetric dimer across the centre of symmetry at ($\frac{1}{2}, \frac{1}{2}, \frac{1}{2}$). The C6–H6 \cdots O3($-x, 1 - y, 1 - z$) interaction forms an $R_2^2(18)$ centrosymmetric dimer across the centre of symmetry at ($0, \frac{1}{2}, \frac{1}{2}$). Together, these interactions form the ladder, which lies in plane (011) and

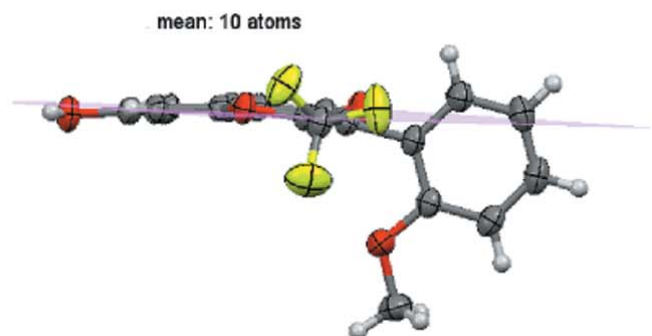


Table 3
Percentages for the most relevant atom–atom contacts in **1**.

H···H'	H···O/O···H	H···F/F···H	H···C/C···H	C···C	C···O/O···C	O···F/F···C	O···O	F···O/O···F	F···F
22.1	18.3	25.1	18.3	6.1	2.3	0.2	3.0	0.8	3.4

which runs parallel to the *a* axis, Fig. 3. There are also C—H··· π interactions present (Table 2).

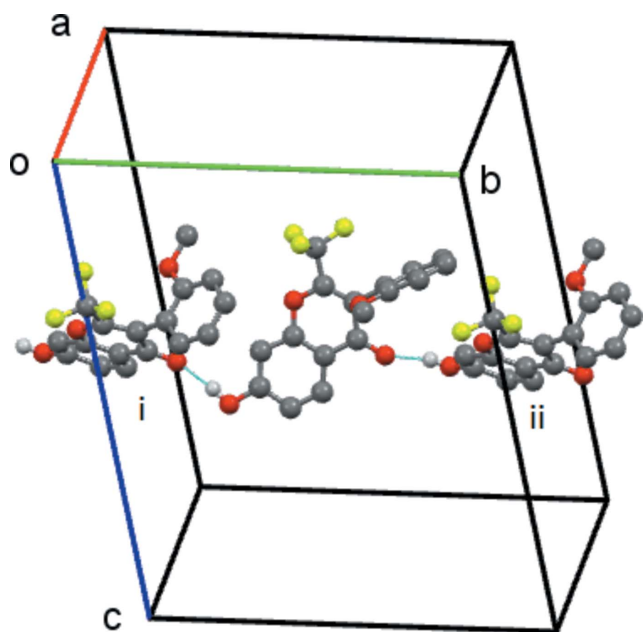


Figure 2
Compound **1**, the simple C8 chain formed by the O7—H7···O4ⁱ hydrogen bond. This chain extends along the *b* axis. Symmetry codes: (i) $-x + \frac{1}{2}, y - \frac{1}{2}, z$; (ii) $-x + \frac{1}{2}, y + \frac{1}{2}, z$. Hydrogen atoms not involved in the hydrogen bonding have been omitted.

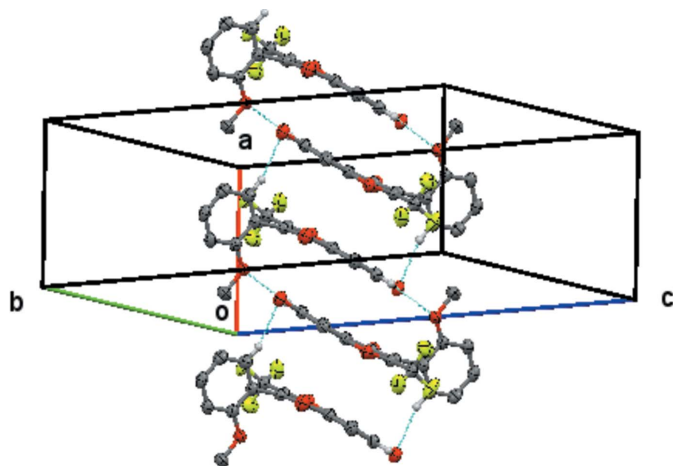


Figure 3
Compound **1**, view of the ladder of alternating linked $R_2^2(18)$ and $R_2^2(20)$ structures formed by the interaction of centrosymmetrically related pairs of C6—H6···O3ⁱⁱ hydrogen bonds across the centre of symmetry at $(0, \frac{1}{2}, \frac{1}{2})$ and centrosymmetrically related pairs of C36—H36···O7ⁱⁱⁱ hydrogen bonds across the centre of symmetry at $(\frac{1}{2}, \frac{1}{2}, \frac{1}{2})$. This chain extends by unit translation along the *a* axis. Hydrogen atoms not involved in the hydrogen bonding have been omitted.

4. Hirshfeld surfaces

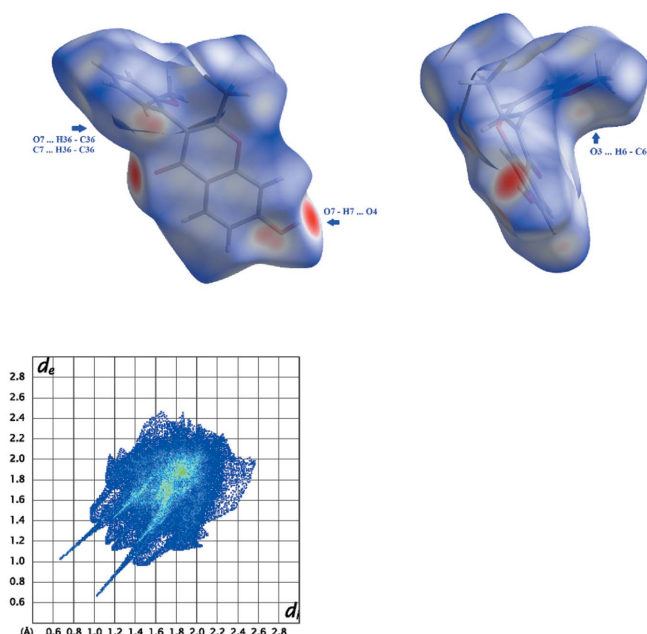
The Hirshfeld surfaces and two-dimensional fingerprint (FP) plots (McKinnon *et al.*, 2004) provide complementary information concerning the intermolecular interactions discussed above. They were generated using *Crystal Explorer 3.1* (Wolff *et al.*, 2012). The Hirshfeld surface mapped over d_{norm} is scaled between -0.250 to 1.200 . The electrostatic potential (ESP) was calculated with *TONTO* (Jayatilaka & Grimwood, 2003) as implemented in *Crystal Explorer 3*.

The contributions from various contacts, listed in Table 3, were selected by the partial analysis of the FP plots. Besides the H···H contacts the other most significant contacts are the H···F/F···H due to the fluorine atoms on the surface. The remaining high percentage contacts are H···O/O···H that include the relevant C—H···O and the O—H···O intermolecular interactions and also the H···C/C···H contacts including C—H···C contacts. The percentage of C···C contacts is 6.1% but they are too long to be considered as π – π stacking. The structure has four oxygen atoms, defining different functional groups, that may act as acceptors for hydrogen bonds: one oxo group, a methoxy group, a hydroxyl group and an alkoxy O atom, all of which participate in short atom–atom contacts with the exception of the chromone alkoxy O atom.

The Hirshfeld surfaces mapped over d_{norm} for **1** (see Fig. 4) show three sets of complementary red spot areas: one of those pairs consist of two intense red areas, circular in shape, that are located near the carbonyl oxygen atom O4 and near the hydroxyl substituent. This close contact accounts for the O4···H7—O7 hydrogen bond as indicated in Fig. 4. Another pair is consists of two light-red areas resulting from the overlap of two red spots near H36 and near the hydroxyl group; they suggest interactions between this hydrogen atom and O7 (that forms a C36—H36···O7 hydrogen contact) and with the carbon atom C7 of the chromone ring (Fig. 5 contains a detail of this contact and the corresponding FP plot area). Finally, there are two complementary very light-red spots of small diameter that suggest the existence of a close contact involving the oxygen atom O3 of the methoxy substituent with hydrogen atom H8 of the chromone ring (O3···H6—C6).

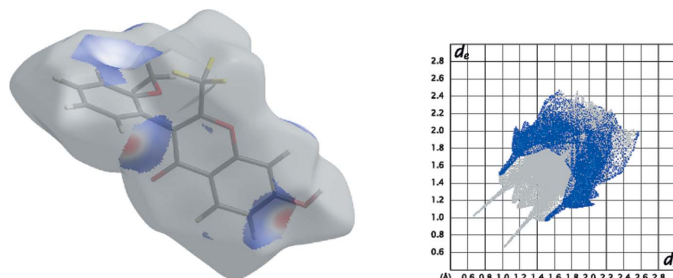
The FP plot for **1** is included in Fig. 4. The light-blue area in the middle of it at d_e/d_i approximately equal to 1.9 \AA shows a higher frequency of the pixels that are due to C···C contacts. The sharp spikes pointing to the southwest are due to O···H contacts and the short wings due to C···H close contacts (see Fig. 5 for details).

In Fig. 6 the mapping of the molecular electrostatic potential (ESP) in the context of crystal packing is shown. As the Hirshfeld surface partitions of the crystal space give non-overlapping volumes associated with each molecule, these

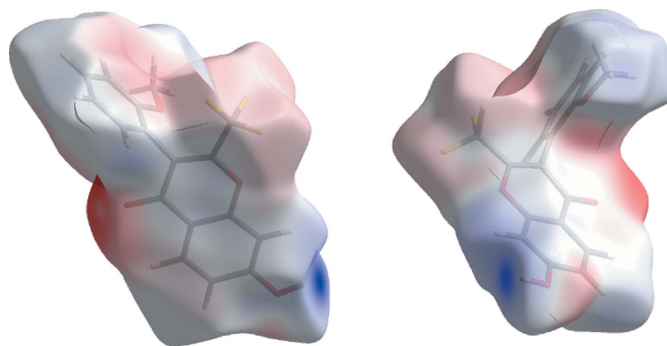

Figure 4

Views of the Hirshfeld surface mapped over d_{norm} for **1** and the corresponding FP plot. The highlighted red spots with large area on the top left image indicate $\text{O} \cdots \text{H}$ contact points involving the carbonyl oxygen atom of the chromone core and the hydrogen atom of the hydroxyl substituent while the pair of superposed light-red spots indicate $\text{C} \cdots \text{H}$ and $\text{O} \cdots \text{H}$ close contacts. The small red-spot areas on the concave and convex face of the right image are due to $\text{C} \cdots \text{H}$ close contacts. The bottom of the figure presents the FP plot for molecule **1**. The light-blue area in the middle of the FP plot at $d_e/d_i \sim 1.9 \text{ \AA}$ shows a higher frequency of the pixels that are due to $\text{C} \cdots \text{C}$ contacts. The sharp spikes pointing to southwest are due to $\text{O} \cdots \text{H}$ contacts; the inner one on the right is related to $\text{O} \cdots \text{H}$ contacts and the short wings due to $\text{C} \cdots \text{H}$ close contacts (see Fig. 5 for details).

surfaces give a kind of ‘electrostatic complementarity’; red areas indicate negative electrostatic potential while blue areas indicate a positive one. The ESP mapped in the Hirshfeld surface for **1** reveals a red area of strongly negative electrostatic potential surrounding the carbonyl region of the chro-


Figure 5

Detail of the FP plot for **1** highlighting the $\text{H} \cdots \text{C}$ contacts (blue) and the corresponding areas in the Hirshfeld surface; The blue area covers the $\text{C} \cdots \text{H}/\text{H} \cdots \text{C}$ close contacts and displays two small wings as well as a pair of short spikes pointing to southwest ending at $(d_e/d_i)/(1.5/1.0) \text{ \AA}$ and *vice versa* that reflect the $\text{C36} \cdots \text{H36} \cdots \text{C7}$ contact area.


Figure 6

The electrostatic potential surfaces for **1** (ranging from -0.0920 to 0.2582 a.u.). The surfaces show the complementarity of electropositive area (blue) near the hydrogen atom of the hydroxyl substituent and red electro-negative area surrounding the vicinity of the lone pairs of the oxo oxygen atom O4.

mone and light red areas surrounding the fluorine atoms of the $-\text{CF}_3$ and as well on the areas covering the oxygen atoms of the hydroxyl and methoxy substituents showing the negative electrostatic potential. The blue region, strongly electropositive, is predominantly located on the hydrogen atom of the hydroxyl substituent and the light electropositive blue patch areas are also surrounding the H atoms of the methoxy substituent and well as H8 and H6 hydrogen atoms of the chromone. The remainder of the Hirshfeld surface is close to neutrality as seen by the grey regions. Thus, the figures highlight the electrostatic complementarity in the $\text{O4} \cdots \text{H7} \cdots \text{O7}$ contact as well as in the $\text{O3} \cdots \text{H6} \cdots \text{C6}$ contact.

5. Database survey

A search made in the Cambridge Structural Database, (Groom *et al.*, 2016), revealed the existence of seven polymorphic and pseudopolymorphic crystal structures of 7-hydroxy-3-phenyl-4*H*-chromen-4-one (Gong *et al.*, 2016). In these structures, the pyran rings are essentially planar. The dihedral angles between the benzopyran ten-membered ring mean plane and the exocyclic benzene ring are given below. KUZJEW, 7-hydroxy-3-phenyl-4*H*-chromen-4-one: 2-methylpropan-2-ol solvate, dihedral angle = $48.28 (7)^\circ$. KUZJIA, 7-hydroxy-3-phenyl-4*H*-chromen-4-one, dihedral angle = $55.23 (8)^\circ$. KUZJIA01, 7-hydroxy-3-phenyl-4*H*-chromen-4-one, dihedral angle = $56.83 (7)^\circ$ (molecule A), $48.27 (6)^\circ$ (molecule B). KUZNIE, 7-hydroxy-3-phenyl-4*H*-chromen-4-one; dimethyl sulfoxide solvate, dihedral angle = $45.91 (7)^\circ$. KUZJUM, 7-hydroxy-3-phenyl-4*H*-chromen-4-one *N,N*-dimethylformamide solvate, dihedral angle = $41.70 (7)^\circ$. KUZKAT, 7-hydroxy-3-phenyl-4*H*-chromen-4-one propan-1-ol, solvate, dihedral angle = $45.18 (9)^\circ$. KUZKEX, 7-hydroxy-3-phenyl-4*H*-chromen-4-one butan-1-ol solvate, dihedral angle = $45.11 (11)^\circ$. In all solvated structures, the 7-OH hydroxyl group is involved in hydrogen bonding with the solvent. In the two KUZJIA(01) structures, $-\text{OH} \cdots \text{O}$ chains are formed as in **1**.

6. Synthesis and crystallization

The title compound was obtained by a two-step synthesis (Balasubramanian & Nair, 2000; Eiffe *et al.*, 2009). Resorcinol and 2-methoxyphenylacetic acid, in equimolar amounts, were suspended in boron trifluoride diethyl etherate (BF₃·Et₂O) and heated at 358 K, for 90 min. Then the mixture was poured into water and stirred until the formation of a solid and extracted with ethyl acetate. The combined organic phases were washed with water, dried over anhydrous sodium sulfate, filtered and evaporated. The product was recrystallized from ethyl acetate solution and used in the subsequent reaction to obtain the isoflavone.

1-(2,4-Dihydroxyphenyl)-2-(2-methoxyphenyl)ethan-1-one (1 mmol), trifluoroacetic anhydride (3 mmol) and trimethylamine (2 ml) were refluxed for 1 h. After cooling, water (15 ml) was added. The solution was acidified (pH 5) with 2 M HCl and stirred at room temperature for 2 h. After extraction with ethyl acetate, the combined organic phases were washed with water, dried over anhydrous sodium sulfate, filtered and evaporated. The isoflavone was recrystallized from ethyl acetate solution. Overall yield: 55%

¹H NMR (DMSO-*d*₆): 3.69 (1H, *s*), 6.95 (1H, *d*, *J* = 2.20 Hz), 7.00 (1H, *ddd*, *J* = 0.97, 7.45, 7.45 Hz), 7.02 (1H, *dd*, *J* = 2.26, 8.82 Hz), 7.09 (1H, *dd*, *J* = 0.90, 8.38 Hz), 7.15 (1H, *dd*, *J* = 1.70, 7.46 Hz), 7.42 (1H, *ddd*, *J* = 1.73, 7.47, 8.31 Hz), 7.92 (1H, *d*, *J* = 8.76 Hz), 11.13 (1H, *s*).

7. Refinement

Crystal data, data collection and structure refinement details are summarized in Table 4. The hydroxyl H atom, H7, was refined isotropically. All other H atoms were treated as riding atoms: C—H = 0.95–0.98 Å with *U*_{iso} = 1.5*U*_{eq}(C-methyl) and 1.2*U*_{eq}(C) for other H atoms.

Acknowledgements

The authors thank the staff at the National Crystallographic Service, University of Southampton, for the data collection, help and advice (Coles & Gale, 2012).

Funding information

This work was supported by the Portuguese Foundation for Science and Technology (FCT) UID/Multi/04546/2013 and FEDER/COMPETE (UID/QUI/UI0081/2013 and POCI-01-0145-FEDER-006980). AG (SFRH/BPD/93331/2013) grant is supported by FCT, POPH and QREN.

References

Balasubramanian, S. & Nair, M. G. (2000). *Synth. Commun.* **30**, 469–484.
 Coles, S. J. & Gale, P. A. (2012). *Chem. Sci.* **3**, 683–689.
 Domenicano, A., Vaciego, A. & Coulson, C. A. (1975). *Acta Cryst.* **B31**, 221–234.
 Eiffe, E., Heaton, A., Walker, C. & Husband, A. (2009). US Patent WO 2009003229 A1.
 Gomes, L. R., Low, J. N., Fonseca, A., Matos, M. J. & Borges, F. (2016). *Acta Cryst.* **E72**, 1121–1125.

Table 4

Experimental details.

Crystal data	
Chemical formula	C ₁₇ H ₁₁ F ₃ O ₄
<i>M</i> _r	336.27
Crystal system, space group	Orthorhombic, <i>Pbca</i>
Temperature (K)	100
<i>a</i> , <i>b</i> , <i>c</i> (Å)	7.9147 (5), 16.2171 (11), 22.5254 (16)
<i>V</i> (Å ³)	2891.2 (3)
<i>Z</i>	8
Radiation type	Mo <i>K</i> α
<i>μ</i> (mm ^{−1})	0.14
Crystal size (mm)	0.21 × 0.07 × 0.01
Data collection	
Diffractometer	Rigaku AFC12
Absorption correction	Multi-scan (<i>CrystalClear-SM Expert</i> ; Rigaku, 2012)
<i>T</i> _{min} – <i>T</i> _{max}	0.775, 1.000
No. of measured, independent and observed [<i>I</i> > 2σ(<i>I</i>)] reflections	35487, 3314, 2777
<i>R</i> _{int}	0.058
(sin θ/λ) _{max} (Å ^{−1})	0.649
Refinement	
<i>R</i> [<i>F</i> ² > 2σ(<i>F</i> ²)], <i>wR</i> (<i>F</i> ²), <i>S</i>	0.036, 0.103, 1.02
No. of reflections	3314
No. of parameters	222
H-atom treatment	H atoms treated by a mixture of independent and constrained refinement
Δρ _{max} , Δρ _{min} (e Å ^{−3})	0.34, −0.21

Computer programs: *CrystalClear-SM Expert* (Rigaku, 2012), *SHELXT* (Sheldrick, 2015a), *OSCAIL* (McArdle *et al.*, 2004), *ShelXle* (Hübschle *et al.*, 2011), *SHELXL2014* (Sheldrick, 2015b), *Mercury* (Macrae *et al.*, 2006) and *PLATON* (Spek, 2009).

Gong, N., Zhang, G., Jin, G., Du, G. & Lu, Y. (2016). *J. Pharm. Sci.* **105**, 1387–1397.
 Groom, C. R., Bruno, I. J., Lightfoot, M. P. & Ward, S. C. (2016). *Acta Cryst.* **B72**, 171–179.
 Hübschle, C. B., Sheldrick, G. M. & Dittrich, B. (2011). *J. Appl. Cryst.* **44**, 1281–1284.
 Jayatilaka, D. & Grimwood, D. J. (2003). *ICCS*, **4**, 142–151.
 Jie Yu, J., Bi, X. J., Yu, B. & Chen, D. (2016). *Nutrients*, **8**, 361–365.
 Macrae, C. F., Edgington, P. R., McCabe, P., Pidcock, E., Shields, G. P., Taylor, R., Towler, M. & van de Streek, J. (2006). *J. Appl. Cryst.* **39**, 453–457.
 McArdle, P., Gilligan, K., Cunningham, D., Dark, R. & Mahon, M. (2004). *CrystEngComm*, **6**, 303–309.
 McKinnon, J. J., Spackman, M. A. & Mitchell, A. S. (2004). *Acta Cryst.* **B60**, 627–668.
 Reis, J., Gaspar, A., Borges, F., Gomes, L. R. & Low, J. N. (2013). *Acta Cryst.* **C69**, 1527–1533.
 Rigaku (2012). *CrystalClear-SM Expert*. Rigaku Corporation, Tokyo, Japan.
 Schepetkin, I. A., Kirpotina, L. N., Khlebnikov, A. I., Cheng, N., Ye, R. D. & Quinn, M. T. (2014). *Biochem. Pharmacol.* **92**, 627–641.
 Sheldrick, G. M. (2015a). *Acta Cryst.* **A71**, 3–8.
 Sheldrick, G. M. (2015b). *Acta Cryst.* **C71**, 3–8.
 Spek, A. L. (2009). *Acta Cryst.* **D65**, 148–155.
 Szeja, W., Grynkiewicz, G. & Rusin, A. (2016). *Curr. Org. Chem.* **21**, 218–235.
 Vitale, D. C., Piazza, C., Melilli, B., Drago, F. & Salomone, S. (2013). *Eur. J. Drug Metab. Pharmacokin.* **38**, 15–25.
 Wolff, S. K., Grimwood, D. J., McKinnon, J. J., Turner, M. J., Jayatilaka, D. & Spackman, M. A. (2012). *Crystal Explorer*. The University of Western Australia.

supporting information

Acta Cryst. (2017). E73, 1130-1134 [https://doi.org/10.1107/S2056989017009896]

Structure of 7-hydroxy-3-(2-methoxyphenyl)-2-trifluoromethyl-4*H*-chromen-4-one

John Nicolson Low, Ligia R. Gomes, Alexandra Gaspar and Fernanda Borges

Computing details

Data collection: *CrystalClear-SM Expert* (Rigaku, 2012); cell refinement: *CrystalClear-SM Expert* (Rigaku, 2012); data reduction: *CrystalClear-SM Expert* (Rigaku, 2012); program(s) used to solve structure: SHELXT (Sheldrick, 2015a); program(s) used to refine structure: *OSCAIL* (McArdle *et al.*, 2004), *ShelXle* (Hübschle *et al.*, 2011) and *SHELXL2014* (Sheldrick, 2015b); molecular graphics: *Mercury* (Macrae *et al.*, 2006); software used to prepare material for publication: *OSCAIL* (McArdle *et al.*, 2004), *SHELXL2014* (Sheldrick, 2015b) and *PLATON* (Spek, 2009).

7-Hydroxy-3-(2-methoxyphenyl)-2-trifluoromethyl-4*H*-chromen-4-one

Crystal data

C₁₇H₁₁F₃O₄

M_r = 336.27

Orthorhombic, *Pbca*

a = 7.9147 (5) Å

b = 16.2171 (11) Å

c = 22.5254 (16) Å

V = 2891.2 (3) Å³

Z = 8

F(000) = 1376

D_x = 1.545 Mg m⁻³

Mo *Kα* radiation, λ = 0.71075 Å

Cell parameters from 31907 reflections

θ = 2.5–27.5°

μ = 0.14 mm⁻¹

T = 100 K

Plate, colourless

0.21 × 0.07 × 0.01 mm

Data collection

Rigaku AFC12

diffractometer

Radiation source: Rotating Anode

Detector resolution: 28.5714 pixels mm⁻¹

profile data from ω-scans

Absorption correction: multi-scan

(*CrystalClear-SM Expert*; Rigaku, 2012)

T_{min} = 0.775, *T_{max}* = 1.000

35487 measured reflections

3314 independent reflections

2777 reflections with *I* > 2σ(*I*)

R_{int} = 0.058

θ_{max} = 27.5°, θ_{min} = 2.5°

h = -10→10

k = -20→20

l = -29→29

Refinement

Refinement on *F*²

Least-squares matrix: full

R[*F*² > 2σ(*F*²)] = 0.036

wR(*F*²) = 0.103

S = 1.02

3314 reflections

222 parameters

0 restraints

Hydrogen site location: mixed

H atoms treated by a mixture of independent

and constrained refinement

w = 1/[σ²(*F_o*²) + (0.0543*P*)² + 1.0823*P*]

where *P* = (*F_o*² + 2*F_c*²)/3

(Δ/σ)_{max} < 0.001

Δρ_{max} = 0.34 e Å⁻³

Δρ_{min} = -0.21 e Å⁻³

Special details

Geometry. All esds (except the esd in the dihedral angle between two l.s. planes) are estimated using the full covariance matrix. The cell esds are taken into account individually in the estimation of esds in distances, angles and torsion angles; correlations between esds in cell parameters are only used when they are defined by crystal symmetry. An approximate (isotropic) treatment of cell esds is used for estimating esds involving l.s. planes.

Fractional atomic coordinates and isotropic or equivalent isotropic displacement parameters (\AA^2)

	<i>x</i>	<i>y</i>	<i>z</i>	$U_{\text{iso}}^*/U_{\text{eq}}$
F21	0.37922 (12)	0.49225 (7)	0.27664 (4)	0.0476 (3)
F22	0.59157 (13)	0.56872 (5)	0.29861 (4)	0.0459 (3)
F23	0.59737 (12)	0.43950 (5)	0.31761 (4)	0.0416 (2)
O1	0.38627 (12)	0.44652 (5)	0.40256 (4)	0.0248 (2)
O3	0.13208 (12)	0.65679 (5)	0.33431 (4)	0.0276 (2)
O4	0.29964 (14)	0.66084 (5)	0.49162 (4)	0.0323 (2)
O7	0.08054 (13)	0.29227 (6)	0.54664 (4)	0.0293 (2)
H7	0.114 (3)	0.2531 (13)	0.5233 (9)	0.055 (6)*
C2	0.42085 (16)	0.52119 (7)	0.37796 (6)	0.0235 (3)
C3	0.38708 (16)	0.59517 (7)	0.40248 (6)	0.0232 (3)
C4	0.31834 (16)	0.59616 (7)	0.46352 (6)	0.0243 (3)
C5	0.17944 (17)	0.50964 (7)	0.54149 (6)	0.0253 (3)
H5	0.1607	0.5575	0.5649	0.030*
C4A	0.26922 (16)	0.51638 (7)	0.48767 (5)	0.0230 (3)
C6	0.11873 (17)	0.43488 (7)	0.56045 (6)	0.0256 (3)
H6	0.0579	0.4311	0.5967	0.031*
C7	0.14709 (17)	0.36333 (7)	0.52579 (6)	0.0248 (3)
C8	0.24070 (17)	0.36720 (7)	0.47361 (6)	0.0244 (3)
H8	0.2647	0.3190	0.4512	0.029*
C8A	0.29805 (16)	0.44429 (7)	0.45536 (5)	0.0224 (3)
C21	0.49789 (19)	0.50614 (7)	0.31732 (6)	0.0277 (3)
C31	0.40573 (17)	0.67677 (7)	0.37198 (6)	0.0244 (3)
C32	0.26803 (16)	0.70816 (7)	0.33969 (5)	0.0237 (3)
C33	0.27695 (18)	0.78732 (8)	0.31499 (6)	0.0274 (3)
H33	0.1837	0.8090	0.2935	0.033*
C34	0.42290 (19)	0.83407 (8)	0.32209 (6)	0.0303 (3)
H34	0.4285	0.8878	0.3055	0.036*
C35	0.56005 (19)	0.80327 (8)	0.35305 (6)	0.0314 (3)
H35	0.6600	0.8352	0.3571	0.038*
C36	0.55002 (18)	0.72477 (8)	0.37832 (6)	0.0290 (3)
H36	0.6433	0.7039	0.4002	0.035*
C321	-0.01472 (19)	0.69009 (9)	0.30555 (7)	0.0343 (3)
H32A	-0.1047	0.6486	0.3052	0.051*
H32B	0.0137	0.7053	0.2647	0.051*
H32C	-0.0533	0.7391	0.3271	0.051*

Atomic displacement parameters (\AA^2)

	U^{11}	U^{22}	U^{33}	U^{12}	U^{13}	U^{23}
F21	0.0446 (6)	0.0703 (7)	0.0280 (5)	0.0018 (5)	-0.0036 (4)	-0.0067 (4)
F22	0.0623 (6)	0.0276 (4)	0.0478 (5)	-0.0090 (4)	0.0258 (5)	-0.0027 (4)
F23	0.0549 (6)	0.0325 (4)	0.0373 (5)	0.0188 (4)	0.0129 (4)	0.0034 (3)
O1	0.0320 (5)	0.0160 (4)	0.0265 (5)	0.0010 (3)	0.0023 (4)	-0.0003 (3)
O3	0.0260 (5)	0.0259 (4)	0.0308 (5)	0.0002 (4)	-0.0032 (4)	0.0043 (4)
O4	0.0432 (6)	0.0178 (4)	0.0357 (5)	-0.0001 (4)	0.0037 (4)	-0.0044 (4)
O7	0.0375 (6)	0.0178 (4)	0.0327 (5)	-0.0016 (4)	0.0040 (4)	0.0008 (4)
C2	0.0248 (6)	0.0188 (6)	0.0269 (6)	0.0001 (5)	-0.0016 (5)	0.0017 (4)
C3	0.0228 (6)	0.0189 (5)	0.0280 (6)	0.0008 (4)	-0.0030 (5)	0.0005 (5)
C4	0.0251 (6)	0.0184 (5)	0.0294 (6)	0.0017 (5)	-0.0031 (5)	-0.0006 (5)
C5	0.0307 (7)	0.0191 (5)	0.0262 (6)	0.0022 (5)	-0.0019 (5)	-0.0027 (5)
C4A	0.0257 (6)	0.0174 (5)	0.0258 (6)	0.0016 (5)	-0.0030 (5)	-0.0012 (4)
C6	0.0299 (7)	0.0223 (6)	0.0245 (6)	0.0027 (5)	0.0006 (5)	-0.0003 (5)
C7	0.0270 (7)	0.0188 (5)	0.0286 (6)	0.0008 (5)	-0.0037 (5)	0.0018 (5)
C8	0.0296 (7)	0.0161 (5)	0.0275 (6)	0.0012 (5)	-0.0022 (5)	-0.0018 (4)
C8A	0.0246 (6)	0.0197 (6)	0.0231 (6)	0.0016 (5)	-0.0017 (5)	-0.0007 (4)
C21	0.0336 (7)	0.0202 (6)	0.0294 (6)	0.0015 (5)	0.0020 (5)	0.0004 (5)
C31	0.0296 (7)	0.0176 (5)	0.0258 (6)	0.0016 (5)	0.0017 (5)	0.0001 (4)
C32	0.0276 (6)	0.0203 (5)	0.0231 (6)	0.0016 (5)	0.0025 (5)	-0.0006 (4)
C33	0.0339 (7)	0.0223 (6)	0.0259 (6)	0.0055 (5)	0.0028 (5)	0.0019 (5)
C34	0.0426 (8)	0.0196 (6)	0.0287 (7)	0.0007 (5)	0.0081 (6)	0.0019 (5)
C35	0.0361 (7)	0.0220 (6)	0.0361 (7)	-0.0056 (5)	0.0043 (6)	-0.0028 (5)
C36	0.0301 (7)	0.0222 (6)	0.0346 (7)	0.0000 (5)	-0.0015 (5)	-0.0007 (5)
C321	0.0292 (7)	0.0375 (7)	0.0362 (7)	0.0034 (6)	-0.0058 (6)	0.0056 (6)

Geometric parameters (\AA , $^\circ$)

F21—C21	1.3314 (17)	C6—C7	1.4164 (17)
F22—C21	1.3256 (15)	C6—H6	0.9500
F23—C21	1.3371 (15)	C7—C8	1.3908 (19)
O1—C2	1.3594 (15)	C8—C8A	1.3921 (17)
O1—C8A	1.3796 (15)	C8—H8	0.9500
O3—C32	1.3662 (15)	C31—C36	1.3895 (19)
O3—C321	1.4356 (16)	C31—C32	1.4057 (18)
O4—C4	1.2340 (15)	C32—C33	1.4008 (17)
O7—C7	1.3514 (15)	C33—C34	1.391 (2)
O7—H7	0.87 (2)	C33—H33	0.9500
C2—C3	1.3475 (17)	C34—C35	1.384 (2)
C2—C21	1.5158 (18)	C34—H34	0.9500
C3—C4	1.4788 (18)	C35—C36	1.3967 (18)
C3—C31	1.4983 (17)	C35—H35	0.9500
C4—C4A	1.4564 (16)	C36—H36	0.9500
C5—C6	1.3723 (17)	C321—H32A	0.9800
C5—C4A	1.4094 (18)	C321—H32B	0.9800
C5—H5	0.9500	C321—H32C	0.9800

C4A—C8A	1.3960 (16)		
C2—O1—C8A	118.46 (9)	F22—C21—F21	107.78 (11)
C32—O3—C321	116.62 (10)	F22—C21—F23	106.92 (12)
C7—O7—H7	107.1 (13)	F21—C21—F23	106.39 (11)
C3—C2—O1	125.88 (12)	F22—C21—C2	112.84 (10)
C3—C2—C21	126.33 (11)	F21—C21—C2	111.33 (12)
O1—C2—C21	107.75 (10)	F23—C21—C2	111.26 (10)
C2—C3—C4	117.63 (11)	C36—C31—C32	119.18 (11)
C2—C3—C31	125.38 (12)	C36—C31—C3	121.91 (12)
C4—C3—C31	116.93 (10)	C32—C31—C3	118.73 (11)
O4—C4—C4A	122.10 (12)	O3—C32—C33	124.28 (12)
O4—C4—C3	122.03 (11)	O3—C32—C31	115.83 (10)
C4A—C4—C3	115.84 (10)	C33—C32—C31	119.89 (12)
C6—C5—C4A	120.84 (11)	C34—C33—C32	119.71 (13)
C6—C5—H5	119.6	C34—C33—H33	120.1
C4A—C5—H5	119.6	C32—C33—H33	120.1
C8A—C4A—C5	117.78 (11)	C35—C34—C33	120.85 (12)
C8A—C4A—C4	120.36 (11)	C35—C34—H34	119.6
C5—C4A—C4	121.66 (11)	C33—C34—H34	119.6
C5—C6—C7	119.78 (12)	C34—C35—C36	119.34 (13)
C5—C6—H6	120.1	C34—C35—H35	120.3
C7—C6—H6	120.1	C36—C35—H35	120.3
O7—C7—C8	122.67 (11)	C31—C36—C35	121.02 (13)
O7—C7—C6	116.44 (12)	C31—C36—H36	119.5
C8—C7—C6	120.88 (11)	C35—C36—H36	119.5
C7—C8—C8A	117.63 (11)	O3—C321—H32A	109.5
C7—C8—H8	121.2	O3—C321—H32B	109.5
C8A—C8—H8	121.2	H32A—C321—H32B	109.5
O1—C8A—C8	116.31 (10)	O3—C321—H32C	109.5
O1—C8A—C4A	120.69 (10)	H32A—C321—H32C	109.5
C8—C8A—C4A	123.01 (12)	H32B—C321—H32C	109.5
C8A—O1—C2—C3	4.95 (19)	C4—C4A—C8A—O1	5.63 (18)
C8A—O1—C2—C21	-172.99 (10)	C5—C4A—C8A—C8	0.76 (19)
O1—C2—C3—C4	5.0 (2)	C4—C4A—C8A—C8	-174.13 (12)
C21—C2—C3—C4	-177.39 (12)	C3—C2—C21—F22	25.4 (2)
O1—C2—C3—C31	-171.91 (12)	O1—C2—C21—F22	-156.64 (11)
C21—C2—C3—C31	5.7 (2)	C3—C2—C21—F21	-95.91 (15)
C2—C3—C4—O4	172.60 (12)	O1—C2—C21—F21	82.03 (13)
C31—C3—C4—O4	-10.19 (19)	C3—C2—C21—F23	145.61 (13)
C2—C3—C4—C4A	-9.24 (17)	O1—C2—C21—F23	-36.46 (15)
C31—C3—C4—C4A	167.97 (11)	C2—C3—C31—C36	-95.96 (16)
C6—C5—C4A—C8A	-1.73 (19)	C4—C3—C31—C36	87.07 (16)
C6—C5—C4A—C4	173.08 (12)	C2—C3—C31—C32	88.86 (16)
O4—C4—C4A—C8A	-177.67 (12)	C4—C3—C31—C32	-88.10 (14)
C3—C4—C4A—C8A	4.17 (18)	C321—O3—C32—C33	-5.40 (18)
O4—C4—C4A—C5	7.6 (2)	C321—O3—C32—C31	175.24 (11)

C3—C4—C4A—C5	-170.51 (12)	C36—C31—C32—O3	178.68 (11)
C4A—C5—C6—C7	0.3 (2)	C3—C31—C32—O3	-6.01 (17)
C5—C6—C7—O7	-178.66 (12)	C36—C31—C32—C33	-0.71 (18)
C5—C6—C7—C8	2.2 (2)	C3—C31—C32—C33	174.60 (11)
O7—C7—C8—C8A	177.81 (12)	O3—C32—C33—C34	-178.71 (12)
C6—C7—C8—C8A	-3.06 (19)	C31—C32—C33—C34	0.63 (18)
C2—O1—C8A—C8	169.42 (11)	C32—C33—C34—C35	0.3 (2)
C2—O1—C8A—C4A	-10.35 (17)	C33—C34—C35—C36	-1.2 (2)
C7—C8—C8A—O1	-178.16 (11)	C32—C31—C36—C35	-0.2 (2)
C7—C8—C8A—C4A	1.6 (2)	C3—C31—C36—C35	-175.30 (12)
C5—C4A—C8A—O1	-179.48 (11)	C34—C35—C36—C31	1.1 (2)

Hydrogen-bond geometry (Å, °)

<i>D</i> —H... <i>A</i>	<i>D</i> —H	H... <i>A</i>	<i>D</i> ... <i>A</i>	<i>D</i> —H... <i>A</i>
O7—H7...O4 ⁱ	0.87 (2)	1.79 (2)	2.6416 (13)	166 (2)
C6—H6...O3 ⁱⁱ	0.95	2.59	3.4309 (16)	148
C36—H36...O7 ⁱⁱⁱ	0.95	2.49	3.3886 (18)	157
C8—H8...Cg3 ^{iv}	0.95	2.93	3.5972 (14)	128
C321—H32b...Cg3 ^v	0.98	2.75	3.6348 (17)	150

Symmetry codes: (i) $-x+1/2, y-1/2, z$; (ii) $-x, -y+1, -z+1$; (iii) $-x+1, -y+1, -z+1$; (iv) $x, -y-3/2, z-1/2$; (v) $x-3/2, y, -z-1/2$.